Local magnetic relaxation and hysteresis in the strong and weak Bose-glass regimes of type-II superconductors: A simple model

M. A. R. LeBlanc, Daniel S. M. Cameron, and David LeBlanc
Department of Physics, University of Ottawa, Ottawa, Ontario, Canada K1N 6N5
(Received 3 January 1997)

We present a simple generic model which reproduces the salient features of the observations of Beauchamp *et al.* [Phys. Rev. B **52**, 13 025 (1995); Phys. Rev. Lett. **75**, 3942 (1995)] on the effect of heavy-ion irradiation on the local magnetic response and relaxation rate of $YBa_2Cu_3O_{7-\delta}$ single crystals. The model assumes that j_c vs H, although altered by the irradiation, remains continuous and the decay rate of the critical currents is diminished below the matching field H_ϕ. [S0163-1829(97)51310-5]

Beauchamp *et al.*[1,2] have recently reported on measurements of the local magnetic response and relaxation rates of untwinned $YBa_2Cu_3O_{7-\delta}$ single crystals as the density of columnar defects is increased. They conclude from their discovery of a peak followed by a valley in the relaxation rate vs magnetic field that the vortex creep rate is (i) appreciably enhanced in the dilute range where the magnetic-flux density $B(x)<B_\phi$, (ii) strongly suppressed in the range $B(x)\approx B_\phi$, and (iii) insensitive to the density of columnar defects when $B(x)>B_\phi$. Here B_ϕ is a flux-line density matching, hence scaling, with the density of columnar defects generated by the heavy-ion irradiation of the specimen. Radzihovsky[3] has developed a theoretical framework which supports these observations. The regimes where $B(x)<B_\phi$, $B(x)>B_\phi$, and $B(x)\approx B_\phi$ are denoted the strong Bose glass, weak Bose glass, and Mott insulator phase, respectively.[1–3] By contrast, Baert *et al.*[4] observe a large peak in flux creep rate when $\langle B\rangle>B_\phi$ in Pb/Ge multilayers with a square lattice of submicron holes, Harada *et al.*[5] observe that the relaxation rate in the irradiated region of $Bi_2Sr_{1.8}CaCu_2O_x$ thin films was less than that in the nonirradiated region, Konczykowski *et al.*[6] find that the creep rate of the remanent flux in $YBa_2Cu_3O_{7-\delta}$ crystals is appreciably decreased by Pb ion irradiation, and Prost *et al.*[7] find a significant decrease of the relaxation rate below 15 K in single crystals of $Bi_2Sr_2CaCu_2O_8$ in fields of 0.2 and 0.5 tesla after irradiation with 5.3 Gev Pb ions along the c axis. The analysis of Khalfin and Shapiro[8] predicts a steplike rise of the magnetic relaxation at high magnetic fields.

In this paper, we present a simple empirical model which (i) successfully reproduces the observations of Beauchamp *et al.*[1,2] on the effect of heavy-ion irradiation on (a) the local magnetic hysteresis and (b) the local magnetic relaxation rates; (ii) is in harmony with the observations of several workers that (a) the enhanced critical current density j_c vs B curves are continuous after heavy-ion irradiation,[9–12] and (b) the flux creep rates are reduced by the heavy-ion irradiation[4–7] in the range $B<B_\phi$; and (iii) makes readily testable predictions.

First, we address the local magnetic hysteresis curves in the context that $B(x)=\mu_0 H(x)$. For simplicity, as in the analysis of Beauchamp *et al.*,[1] we consider infinite slab geometry where the applied magnetic field H_a is directed parallel to the surfaces situated at $x=0$ and $x=2X$. By symmetry, we can focus on the space $0\leqslant x\leqslant X$.

We assume that the field profiles initially exist in a critical state, hence Maxwell's equation reads $dH/dx=\pm j_c(H(x))$. Beauchamp *et al.*[1] exploited a modified Bean model where the structure observed in the local magnetic hysteresis of the irradiated specimens corresponds to B_ϕ. In their model, the critical current density $j_c=j_{c1}$ when $B(x)<B_\phi$, $j_c=j_{c2}$ when $B(x)>B_\phi$, and j_c rapidly descends from j_{c1} to j_{c2} in the vicinity of B_ϕ.

In crucial contrast with their model, we assume that j_c vs H is continuous both before and after irradiation. For purpose of illustration, we choose the well-known Kim expression[13] in the form

$$j_c=\frac{j_0 H_{\text{ref}}}{\{H(x)+H_0\}}\,n, \tag{1}$$

where the current density parameter j_0 and the parameter H_0 are viewed as quantities which can be dramatically affected by the heavy-ion irradiation, whereas the reference field H_{ref} and the exponent n characterizing the specimen are taken to be insensitive to this process.

We note that Eq. (1) with $n=1$ emerges from the data of Krusin-Elbaum *et al.*,[12] the simulation experiment by Reichhardt *et al.*[14] on the dynamics of vortices interacting with columnar defects, and the Bose-glass theoretical analysis of Nelson and Vinokur.[15] Also, Eq. (2) with $n=2$ fits the measurements of Gerhaüser *et al.*[10] on the effect of heavy-ion irradiation on j_c.

We visualize critical states where the induced persistent currents are unidirectional in the half-space $0\leqslant x\leqslant X$ and focus on the field profiles where H_a is positive ascending or descending in magnitude (see Fig. 1). Introducing Eq. (1) (where to fix ideas, we let $n=1$) into Maxwell's equation and integrating leads to

$$H(x)=\{(H_a+H_0)^2\pm 2j_0H_{\text{ref}}x\}^{1/2}-H_0, \tag{2}$$

where the + sign applies when H_a is descending in magnitude and the − sign in the space where $H(x)$ is positive when H_a is ascending in magnitude. In the space $x_0\leqslant x\leqslant X$ where $H(x)$ is negative (see Fig. 1),

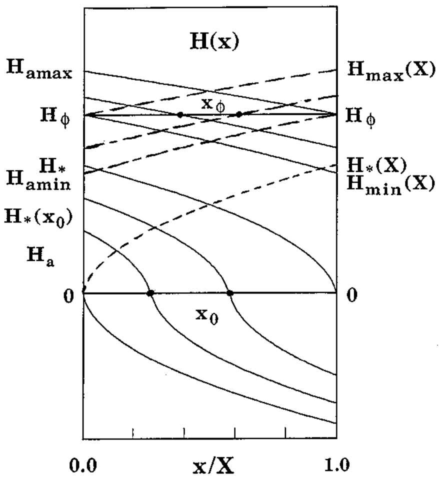

FIG. 1. Displays critical field profiles with H_a increasing (solid lines) and decreasing (dashed lines) in magnitude. The profiles were calculated using $j_c = j_0 H_{\mathrm{ref}}/[H(x)+H_0]$ with the parameters listed in the caption of Fig. 2 under j_c'''. The profiles should be compared with Fig. 3 of Ref. 1 and Fig. 1 of Refs. 16 and 17.

$$H(x) = -\{2j_0 H_{\mathrm{ref}}(x-x_0)+H_0^2\}^{1/2}+H_0, \tag{3}$$

where $H(x_0)=0$ in Eq. (2) leads to $x_0=\{(H_a+H_0)^2 - H_0^2\}/2j_0H_{\mathrm{ref}}$.

Figure 2(a) displays the evolution of the hysteresis curves at the center of the specimen as the heavy-ion irradiation modifies the dependence of j_c on H as shown in the inset by altering the parameters j_0 and H_0. Figure 2(b) displays hysteresis curves for different distances from the surface for the outermost hysteresis curve and uppermost inset of Fig. 2(a). Clearly, the families of calculated hysteresis curves presented in our Fig. 2 reproduce the major features of the corresponding data of Beauchamp *et al.*[1,2] We stress that (i) the $j_c(H)$ curves introduced in this analysis are continuous, and (ii) the matching field H_ϕ plays no explicit role in the structure of j_c vs H, hence in the structure of $H(x)$ vs H_a. (i) and (ii) therefore differ radically from the assumption of Beauchamp *et al.*[1] that j_c vs H exhibits an abrupt descent when $H \approx H_\phi$.

The steep slopes in their $H(x)$ vs H_a curves[1] are directly associated with H_ϕ. In our model, $[dH(x)/dH_a]_{x=x_0} = [H_*(x_0)+H_0]/H_0$ becomes very steep as H_0 is made to diminish by irradiation. $H_*(x_0)=H_a=(H_0^2+2j_0H_{\mathrm{ref}}x_0)^{1/2} - H_0$. Note also the symmetry and relationship of the four points in the hysteresis curves of Fig. 2 where $H(x)$ crosses the vertical and horizontal coordinate axes, i.e., $H(x) = H_*(x_0)$ when $H_a=0$, and $H_a=H_*(x_0)$ when $H(x)=0$.

We now turn to the effect of the irradiation on the local magnetic relaxation rates. We apply the normalized relaxation rate of Beauchamp *et al.*[2] in the form

$$S_n = \left\{ \frac{-1}{M(x)} \right\} \frac{dH(x)}{d\ \ln t} = \left\{ \frac{-1}{M(x)} \right\} \frac{dH(x)}{d(j/j_0)} \frac{d(j/j_0)}{d\ \ln t}, \tag{4}$$

where $M(x)=H(x)-H_a$. Adopting the approach of several workers,[18–21] we assume that, (i) only the parameter j_0 changes with time in Eq. (1), hence in Eqs. (2) and (3),

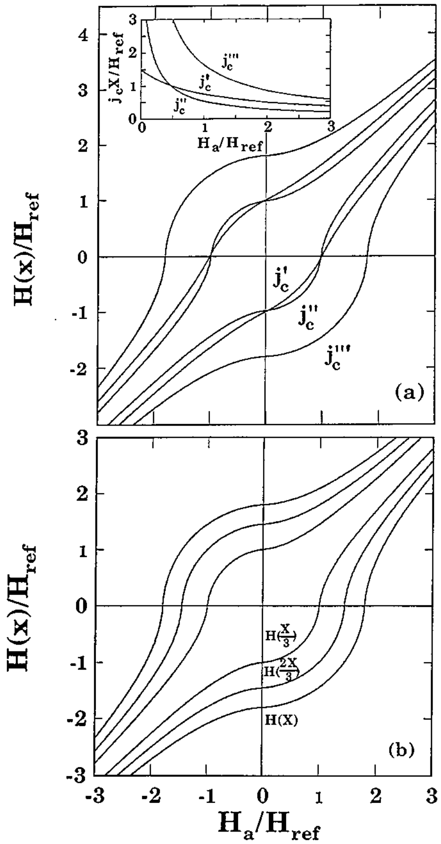

FIG. 2. (a) Displays hysteresis curves of $H(x)$, the magnetic field at the center of the specimen vs H_a, the applied magnetic field, calculated using $j_c=j_0H_{\mathrm{ref}}/[H(x)+H_0]$ shown in the inset with j_0X/H_{ref}= 1.5, 0.6, and 1.8, and H_0/H_{ref}= 1.0, 0.12, and 0.10 for $j_c = j_c'$, j_c'', and j_c'''. Taking $\mu_0 H_{\mathrm{ref}} \approx 1.5$ T gives a good fit to Fig. 1 of Ref. 2. (b) Displays local hysteresis curves $H(x)$ for different distances from the surface (x/X=1/3, 2/3, and 1 for the inner, middle, and outer curves) calculated using j_c'''.

and (ii) $d(j/j_0)/d\ \ln t$ does not depend on H. We focus on the initial values of the decay rates, $R_n = |dH(x)/d(j/j_0)/M(x)|$.

The insets of Figs. 3 and 4 display R_n vs H_a and vs $H(x)$ for the three cases already illustrated in Fig. 2. The dramatic peaks of height, $R_{n\mathrm{peak}}=j_0x/H_0H_*(x_0)$, occurring at $H_a = H_*(x_0)$, hence at $H(x_0)=0$, arise from the feature that j_c vs H of Eq. (1) is convex downwards when $n>0$. Other dependences of j_c on H with this property such as $j_c = j_0 e^{-H/H_0}$, and $j_c = j_0\{1-(H/H_{c2})\}^m$ where $m>1$, also give rise to such a peak in our framework. We stress that in our model H_ϕ plays no explicit role in the existence of this local relaxation peak.

To account for the valley in the local relaxation rates discovered by Beauchamp *et al.*,[2] we now amend the above assumption that $d(j/j_0)/d\ \ln t$ is independent of $H(x)$. In harmony with the observations of several workers,[4–7] we envisage that $d(j/j_0)/d\ \ln t$ is smaller in the regions where $H(x)<H_\phi$ than in the regions where $H(x)>H_\phi$. For simplicity, we assume an abrupt change in this quantity at $H(x)=H_\phi$. Consequently we write $d(j_1/j_{01})/d\ \ln t = fd(j_2/j_{02})/d\ \ln t$ where f is a temperature-dependent parameter lying between 0 and 1. Here, for bookkeeping clarity,

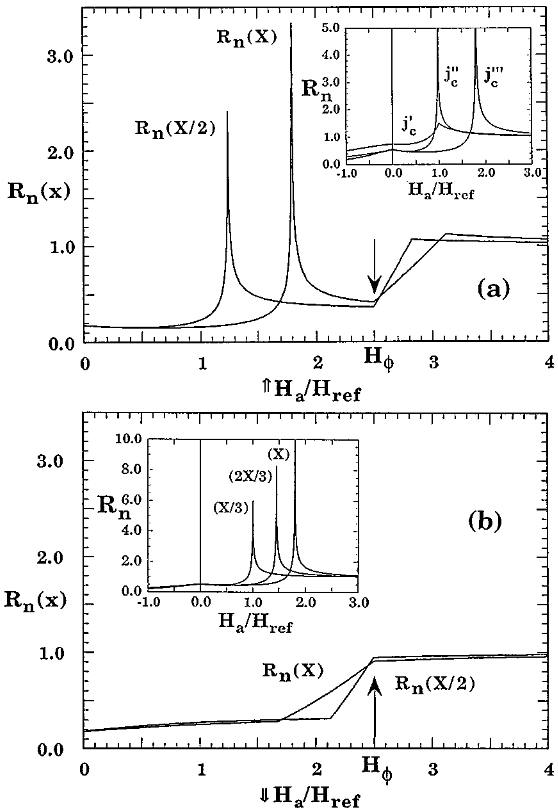

FIG. 3. Displays the initial local decay rates defined in the text, where $d(j/j_0)/d\ln t$ for the field profiles $H(x)<H_\phi$ is a fraction $f=1/3$ of that where $H(x)>H_\phi$ vs H_a, increasing (a) and (b) decreasing in magnitude. The curves are calculated using j'''_c for $x/X=1$ and 1/2. The lower and upper boundaries of the nearly linear slope are situated at H_ϕ and $H_{a\max}=\{(H_\phi+H_0)^2+2j_0H_{\rm ref}x_m\}^{1/2}-H_0$ for (a), and at $H_{a\min}=\{(H_\phi+H_0)^2-2j_0H_{\rm ref}x_m\}-H_0$ and H_ϕ for (b). The peaks appear at $H_a=H_*(x_0)=H_*(x_m)=(H_0+2j_0H_{\rm ref}x_m)^{1/2}-H_0$ with height $R_{nf\rm peak}=fj_0x_mH_{\rm ref}/H_0H_*(x_0)$. Here x_m denotes the position of the field measuring probe. The upper inset displays the local decay rate R_n at $x=X$ calculated using j'_c, j''_c, and j'''_c when $d(j/j_0)/d\ln t$ is the same whether $H(x)\gtrless H_\phi$, hence $f=1$. The lower inset complements the upper inset by displaying $R_n(x)$ calculated at $x=X=1/3$, 2/3, and 1 for j'''_c. The curves in (a) and (b), taking $\mu_0H_{\rm ref}\approx1.0$ T, $H_\phi/H_{\rm ref}=2.5$, should be compared with that of Fig. 2 of Ref. 2 (note the crystal here is different from that of their Figs. 1 and 3). Also compare (b) with Figs. 2(b) and 3(b) of Ref. 4 [our model does not show a descent near H_{c2}, since this quantity has not been introduced into our formula for $j_c(H)$].

j_{01} denotes j_0 where $H(x)<H_\phi$, and j_{02} denotes j_0 where $H(x)>H_\phi$. We stress however that $j_{01}=j_{02}=j_0$.

For the field profiles where $H(x)<H_\phi$ for $0\leqslant x\leqslant X$, we now write $R_n=R_{nf}=|f\,dH(x)/d(j_1/j_{01})/M(x)|$. The field profiles which intersect the field boundary H_ϕ now read, in the space, $x_\phi<x\leqslant X$ (see Fig. 1), before the relaxation begins

$$H_i(x)=\{(H_\phi+H_0)^2\mp2j_{0i}H_{\rm ref}(x-x_{\phi i})\}^{1/2}-H_0, \tag{5}$$

$$x_{0i}=\{\pm(H_a+H_0)^2\mp(H_\phi+H_0)^2\}/2j_{0j}H_{\rm ref}, \tag{6}$$

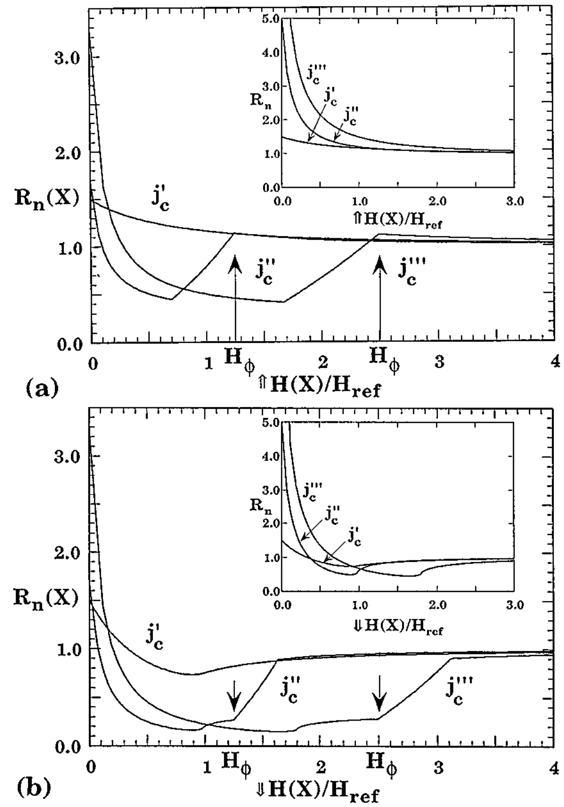

FIG. 4. Complements Fig. 3. In the main figures, the decay rates calculated using j'_c, j''_c, and j'''_c and with $f=1/3$ are displayed vs $H(x)$ increasing in magnitude in (a), and decreasing in magnitude in (b). Figure (a) with $\mu_0H_{\rm ref}\approx1.5$ T, $H_\phi/H_{\rm ref}=0$, 1.25, and 2.5 should be compared with Fig. 3 of Ref. 2. The lower and upper boundaries of the nearly linear slope are situated at $H(x_m)_{\min}=H_{a\min}$ and H_ϕ for (a) and at H_ϕ and $H(x_m)_{\max}=H_{a\max}$ for (b). The peaks at $H(x)=0$ have a height, $R_{nf\rm peak}=fj_0x_mH_{\rm ref}/H_0H_*(x_0)$ as in Fig. 3. The insets complement the corresponding main figures by displaying the decay rates vs $H(x)$ with $d(j/j_0)/d\ln t$ the same whether $H(x)\lesseqgtr H_\phi$ (hence here $f=1$).

where for H_a ascending in magnitude, $i=1$ and $j=2$ and the upper signs apply, while for H_a descending in magnitude, $i=2$ and $j=1$ and the lower signs apply. The decay rate R_{nf} in the space $x_\phi<x\leqslant X$ for these two situations, now reads

$$R_{nfk}=\left|\frac{1}{M(x)}\frac{dH_k}{d(j/j_0)}\right| =\left|\frac{1}{M(x)}\left\{f\,\frac{\partial H_k}{\partial(j_1/j_{01})}+\frac{\partial H_k}{\partial(j_2/j_{02})}\right\}\right|, \tag{7}$$

where now the subscript $k=1$ denotes $H_1(x)$ and $k=2$ denotes $H_2(x)$.

The ensuing relaxation rates vs H_a and $H(x)$ ascending and descending in magnitude are displayed in the main parts of Figs. 3 and 4. Clearly, these theoretical curves reproduce the salient features of the corresponding data curves of Beauchamp *et al.*[2] We note that our model generates a ''rise'' or ''drop'' in the vicinity of H_ϕ whether H_a and $H(x)$ are ascending or descending in magnitude. These structures are illustrated in the main parts of Figs. 3 and 4 and their boundaries are given in the captions of these figures. In the framework of our model, the data of Beauchamp *et al.*[2] indicate that $d(j/j_0)/d\ \ln t$ in the range of $H(x) > H_\phi$ is insensitive to the irradiation since we obtain agreement with their measurements of the evolution of S_n vs irradiation although our model addresses $R_n = S_n/d(j/j_0)/d\ \ln t$ [compare the high-field region of our Fig. 4(a) with that of Fig. 3 of Ref. 2].

We have proposed a simple generic empirical model which reproduces the local hysteresis curves observed by Beauchamp *et al.*[1,2] and provides an account of the peak and valley they found in the local magnetic relaxation rates of their specimens subjected to heavy-ion irradiation. Our analysis predicts that a peak in local magnetic relaxation will appear at $H_a = H_*(x_0)$ in graphs of the rate of decay vs H_a and at $H(x) = 0$ in *all* specimens which exhibit a convex downwards curve for j_c vs H. We note that our model also applies to idealized cylindrical geometry simply by replacing x/X in our formulas by $[1-(r/R)]$. Finally, we recommend that workers display $S = dH(x)/d\ln t$ rather than the *composite* quantity S_n.

[1] K. M. Beauchamp *et al.*, Phys. Rev. B **52**, 13 025 (1995).
[2] K. M. Beauchamp *et al.*, Phys. Rev. Lett. **75**, 3942 (1995).
[3] L. Radzihovsky, Phys. Rev. Lett. **74**, 4919 (1995).
[4] M. Baert *et al.*, Phys. Rev. Lett. **74**, 3269 (1995).
[5] K. Harada *et al.*, Phys. Rev. B **53**, 9400 (1996).
[6] M. Konczykowski *et al.*, Phys. Rev. B **44**, 7167 (1991).
[7] D. Prost *et al.*, Phys. Rev. B **47**, 3457 (1993).
[8] I. B. Khalfin and B. Ya. Shapiro, Physica C **207**, 359 (1993).
[9] L. Civale *et al.*, Phys. Rev. Lett. **67**, 648 (1991).
[10] W. Gerhaüser *et al.*, Phys. Rev. Lett. **68**, 879 (1992).
[11] R. C. Budhani, M. Suenaga, and S. H. Liou, Phys. Rev. Lett. **69**, 3816 (1992).
[12] L. Krusin-Elbaum *et al.*, Phys. Rev. B **53**, 11 744 (1996).
[13] Y. B. Kim, C. F. Hempstead, and A. R. Strnad, Phys. Rev. Lett. **9**, 306 (1962); Phys. Rev. **129**, 528 (1963); **131**, 2486 (1963).
[14] C. Reichhardt *et al.*, Phys. Rev. B **53**, 8898 (1996).
[15] David R. Nelson and V. M. Vinokur, Phys. Rev. B **48**, 13 060 (1993).
[16] M. Konczykowski *et al.*, Physica C **235-240**, 2965 (1994).
[17] R. A. Richardson, O. Pla, and F. Nori, Phys. Rev. Lett. **72**, 1268 (1994).
[18] Y. Yeshurun *et al.*, Phys. Rev. B **38**, 11 828 (1988).
[19] Donglu Shi *et al.*, Phys. Rev. B **42**, 2062 (1990).
[20] Ming Xu *et al.*, Phys. Rev. B **43**, 13 049 (1991).
[21] Yang Ren Sun *et al.*, Physica C **194**, 403 (1992).